

Dispersive Switching in Bistable Models

H. A. Batarfi,

Mathematics Department, Faculty of Science, King Abdulaziz University
(Women's Campus),

P.O. Box 41101 Jeddah 21521 Kingdom of Saudi Arabia.

E-mail: hatarfi@kau.edu.sa

Novel switching processes in optical bistable models of homogeneously or inhomogeneously broadened 2-level atoms placed in ring cavity with atoms in contact with normal or squeezed vacuum reservoirs are investigated. This is done through computational examination of the relevant input-output relationship by *simultaneously* varying the atomic and cavity detuning parameters for fixed values of the input laser field.

Keywords nonlinear optical process: switching.

1 Introduction

In optics, bistable behaviour of a physical system is mainly due to a device (driven optical cavity) filled with a nonlinear medium together with the action of a feedback process (provided by the cavity mirrors). For proper choice of the system parameters, the input-output field relationship exhibits bistable (or multistable) behaviour. Such a bistable device with certain nonlinear materials has many potential applications[1,2] among which is the switching operation (switch-on and -off) between the two stable states of the output field.

The *basic* optical bistable (OB) absorptive model of homogeneously 2-level atoms placed in a ring cavity at exact atomic and cavity resonances (i.e. all three frequencies of atomic transition, input laser field and the single cavity mode are equal) has been analysed by Bonifacio and Lugiato[3]. This was subsequently generalised[4,5] to include the dispersive effects (i.e. both atomic transition and cavity mode frequencies are detuned from the input field frequency)- as well the inhomogeneous broadening of the atomic transition. Regions of bistability were identified analytically for non-zero values of the cavity and atomic detuning parameters.

In the case where the 2-level atoms is in interaction with a broadband squeezed vacuum (SV) field the authors of [6]-also see [7]- investigated the "*phase switching*" effect where for fixed values of the input field and by varying the phase of the SV

field the output field exhibits either one-way or 2-way switching effect. Also, for a mesoscopic (non-dissipative) multistable system[8,9], it has been shown that for a fixed value of the input field and by varying the atomic cooperative parameter (C) (which comprises the atomic density) the output field exhibits multiple "cooperative switching". Similar cooperative switching process for OB model of dissipative 2-level atoms in the normal vacuum (NV) and SV fields has been analysed in[10].

In our presentation, we investigate further switching effect, namely, the "dispersive switching" in the output field at fixed value of the input field by varying *simultaneously* both atomic and cavity detunings with the same amount (same or opposite sign). We examine the two main OB models of homogeneous 2-level atoms in NV and SV fields. The case of inhomogeneous broadening is also examined.

2 Homogeneously broadened atoms

2.1 Normal Vacuum Case:

For the OB model of homogeneously broadened 2-level atoms in a ring cavity (or Fabry-cavity) within the spatial mean field approximation and for non-zero atomic and cavity detunings the characteristic input-output field relation is of the normalised form [4,5],

$$Y = \frac{X}{(1 + \delta^2 + X)^2} \left[(1 + \delta^2 + X + 2C)^2 + (\theta (1 + \delta^2 + X) - 2C\delta)^2 \right] \quad (1)$$

The notations are: X , Y are the dimensionless output and input field intensities respectively. C is the cooperative parameter, θ and δ are the normalised cavity and atomic detuning parameters respectively.

Now, we observe that for $\theta = \lambda\delta$, where λ is a +ve or -ve number, equ(1) is a cubic equation in δ and hence for fixed values of Y and certain range of δ , the output field X will show a bistable behaviour and hence switching effect. Since both X and δ in equ(1) (for $\theta = \lambda\delta$) occur as cubics, it is not easy to analyse mathematically the range in which switching effect may occur. Hence our investigation is computational just as in the SV case [6,7].

The 3D plot of (Y, X, δ) for $C = 5$, $\theta = \delta$ is given in Fig(1a). The contour plot of X with δ to be referred to as *dispersive switching diagram*, at fixed input field $Y = 35$ is given in Fig(1b): as inverted omega or mushroom shape. In this case we have two

bistable regions in the interval $0.28 < |\delta| < 0.56$. If we plot the input-output field (X, Y) at fixed $\theta = \delta = 0.5$ (Fig(1c)) then at $Y = 35$, X has two stable (lower and upper) values corresponding to points P_1, P_2 (the point P_2 is unstable). Fig(1b) shows how these points move as δ varies. As δ increases, P_1 moves until it reaches the unstable point A_1 and the system then switches on to the stable right upper branch and staying on that branch with further increase in δ .

Note, if at the point P_2 in Fig(1b), δ decreases then the system similarly switches-on at A_2 to the stable left upper branch. The movement of point P_3 on the upper branch in Fig(1b) shows that the system will switch-down at A_3 , to the stable lower branch-but the further decrease in δ will cause the system to switch-up at A_2 to the upper left stable branch. Hence, we have two-way dispersive switching effect.

For increasing value of $C = 10$, $\theta = \delta$, Fig(2) shows the corresponding behaviour, where the 3D plot shows a pronounced peak, and for fixed $Y = 90$, the switching diagram shows only one-way switching (switch-up): The point P_1 on the isle in Fig(2b) moves to the unstable point $A_1(A_2)$ by increasing (decreasing) the value of δ where the system switches up to the single stable upper branch. The movement of the point P_3 on the upper branch will only cause a change in X with peak value at $\delta = 0$ but no jumping effect occurs. For $\theta = -\delta$ the corresponding dispersive switching diagram for $C = 5, 10$, Figs(3a,b), are essentially the inverse of Figs(1b,2b) with qualitative difference for the fixed values of Y and the stable lower branch in Fig(2b) is almost flat.

2.2 Squeezed Vacuum Case:

In the case where the 2-level atoms are in contact with SV field, the characteristic relation(1) is generalised to [6,7]:

$$Y = \frac{X}{(1 + \delta^2 + b_1 X)^2} \left[(1 + \delta^2 + b_1(X + 2C))^2 + (\theta(1 + \delta^2 + b_1 X) - 2Cb_2)^2 \right] 2 \quad (2)$$

where $b_1 = 1 - \frac{2|M|}{1+2N} \cos(\phi)$, $b_2 = \frac{\delta+2M \sin(\phi)}{1+2N}$, $\phi = \phi_s - 2\phi_f$ is the relative phase of the SV field, with respect to the input field. The SV parameters N (average photon number) and $M = |M|e^{i\phi}$ (degree of squeezing) are related by $|M|^2 = N(N+1)$ for ideal squeezing.

In Fig(4a), we show the dispersive switching diagram for $C = 10$, $N = 0.1$, $\phi = 0$, $\theta = \delta$ at fixed $Y = 70$, with $(X - Y)$ relation at $\theta = \delta = 0$ shown in Fig(4b).

The movement of P_1 as δ increases will lead to switch-up at the unstable point A_1 to the right upper stable branch where further increase in δ results in decrease of X but decreasing δ will lead to switch-down at A_2 to the stable lower branch. As for point P_3 on the isolated isle, the increase or decrease in δ will result in switching-down process to the stable lower branch where further increase (or decrease) in δ will lead again to switch-up at point A_1 (or A_3). For larger value of $Y = 72$, the switching-diagrams in Fig(4c) shows the merger of the isolated isle (Fig(4a)) which results in multiple switch-up and -down processes. For $Y = 80$, Fig(4d), shows two isolated isles underneath a continuous stable upper branch with possible switch-up processes *only*. In all these cases, the switching diagram is symmetric with respect to δ . Changing the SV phase to $\phi = \frac{\pi}{2}$ makes the switching diagram asymmetric in δ (Figs(5)). The case of $\theta = -\delta$ with $\phi = \frac{\pi}{2}$ and $Y = 80$ has the effect to isolate an asymmetric island around $\delta = 0$ (Fig.6a) to induce one-way switching down effect. Increasing Y to 100 causes the merge of this island with the lower stable branch and results in an asymmetric switching diagram of two-way (up and down) effect (Fig.6b).

3 Inhomogeneously broadened atoms

In the case of inhomogeneously broadened 2-level atoms with Lorentzian distribution of peak (central) frequency ω_a , the input-output field relation in the general case of SV field is of the form [10],

$$Y = X \left[\left(1 + 2C \frac{b_1 (\sigma' + g_1)}{g_1 g_2} \right)^2 - \left(\theta + 2C \frac{(b_3 - b_2 g_1)}{g_1 g_2} \right)^2 \right] \quad (3)$$

where: $g_1 = g_1(X) = \sqrt{1 + b_1 X}$, $g_2 = g_2(X) = \delta^2 + (\sigma' - g_1(X))$, $b_{1,2}$ are defined below equ(2), $b_3 = \frac{2M \sin(\phi)}{1+2N}$, σ' is the normalised Lorentzian width; and δ is now the atomic detuning (i.e. the difference between the (atomic) peak frequency ω_a and ω_L the (laser) input field frequency.

In the case of Normal vacuum ($b_1 = 1$, $b_2 = \delta$, $b_3 = 0$) we have obtained a qualitative dispersive switching diagram similar to that obtained in the homogeneous case. The search in the SV case for $\sigma' = 1$, $\theta = -\delta$, $\phi = \frac{\pi}{2}$, $N = 0.1$ shows that the dispersive switching diagram has asymmetric *double* OB shape. Fig(8).

Figure 1: The time evolution of the

4 Summary

We have computationally explored the possibility of a new switching effects in OB models of 2-level (homogeneously/inhomogeneously broadened) atoms in the presence of normal or squeezed vacuum (SV) fields. This is done for certain input field values by simultaneously varying atomic and cavity detuning (δ, θ) such that $\theta = \lambda\delta$, with λ constant. The switching diagram (output field vs. dispersive detuning) exhibits a rich of possible one-, two-, multiple-switching process and even double bistable behaviour in the inhomogeneously broadened case with SV field.

Thus a single dispersive control (as a result of linearly and simultaneously changing both atomic and cavity detunings) offers interesting manipulation of switching effects in optical bistable devices.

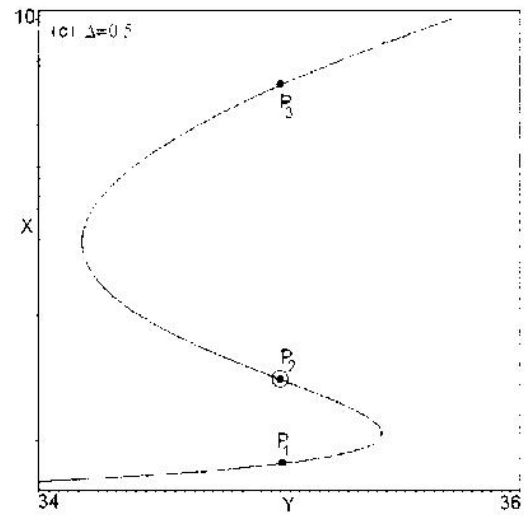
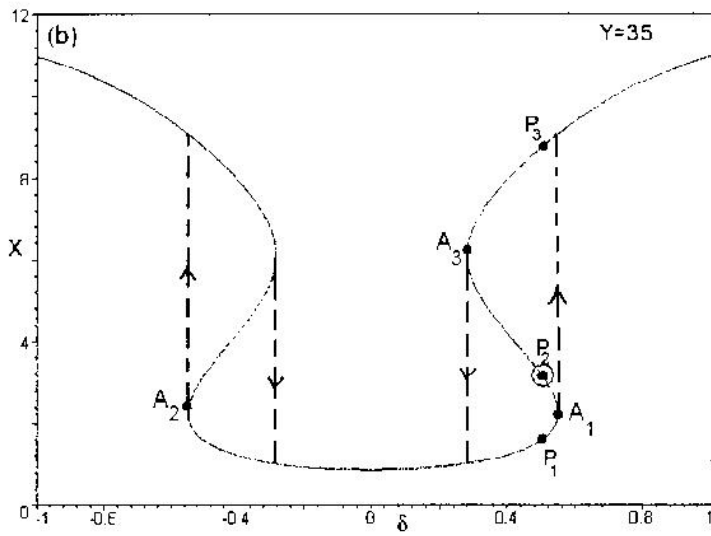
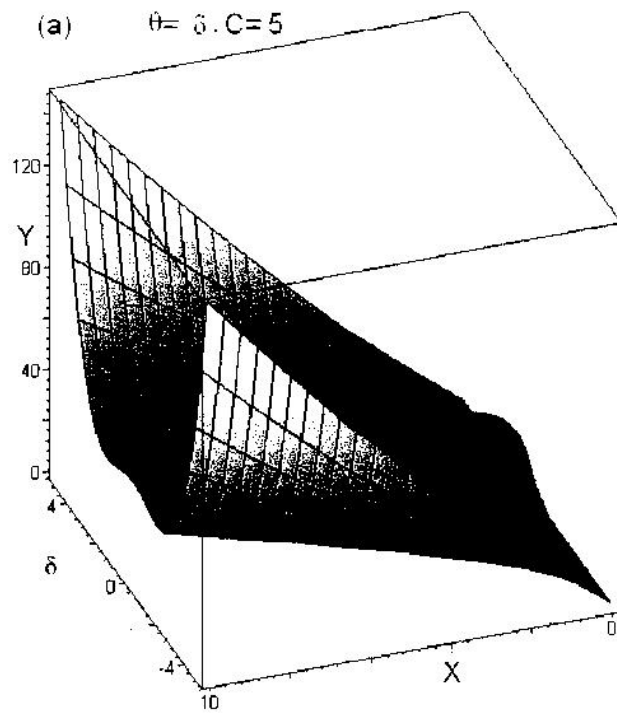
Acknowledgement

The author wishes to present her thanks to Prof. S. S. Hassan (University of Bahrain) for his fruitful comments.

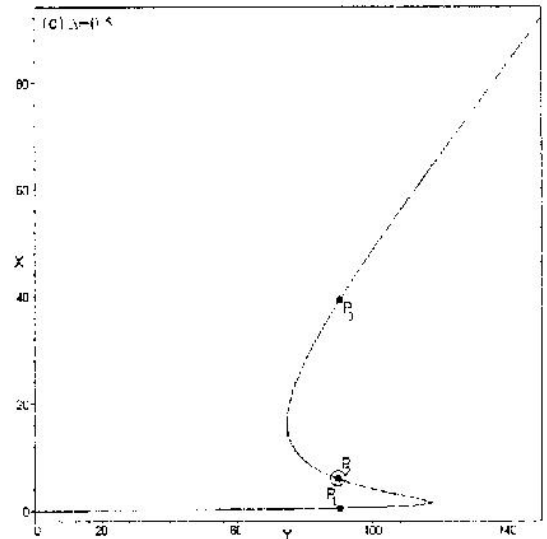
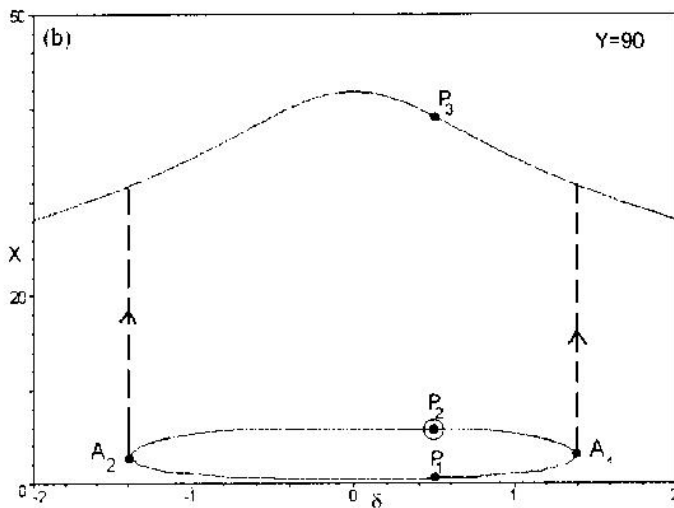
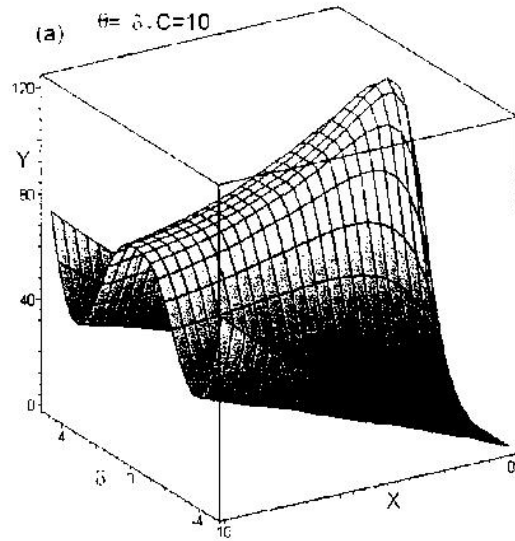
References

- [1] H.M. Gibbs, S. L. McCall and T.N.C. Venkatesan, *Phys. Rev. Lett.* **36** (1976)1135
- [2] E. Abraham and S.D. Smith, *Rep. Prog. Phys.* **45** (1982) 815; P. W. Smith, ed. Special issue on Optical Bistability, *I.E.E.E. J. Q-Electr. QE-* **17** (1981); C. M. Bowden, M. Ciftan and H. R. Robl, eds, *Optical Bistability*, (Plenum Press, N.Y.,1981).
- [3] R. Bonifacio and L. A. Lugiato, *Opt. Commun.* **19** (1976) 172; *Phys. Rev. A* **18** (1978) 1129.
- [4] S. S. Hassan, P. D. Drummond and D. F. Walls, *Opt. Commun.* **27** (1978) 480.
- [5] R. Bonifacio, L. A. Lugiato, *Lett. Nuovo Cimento* **21** (1978) 510.

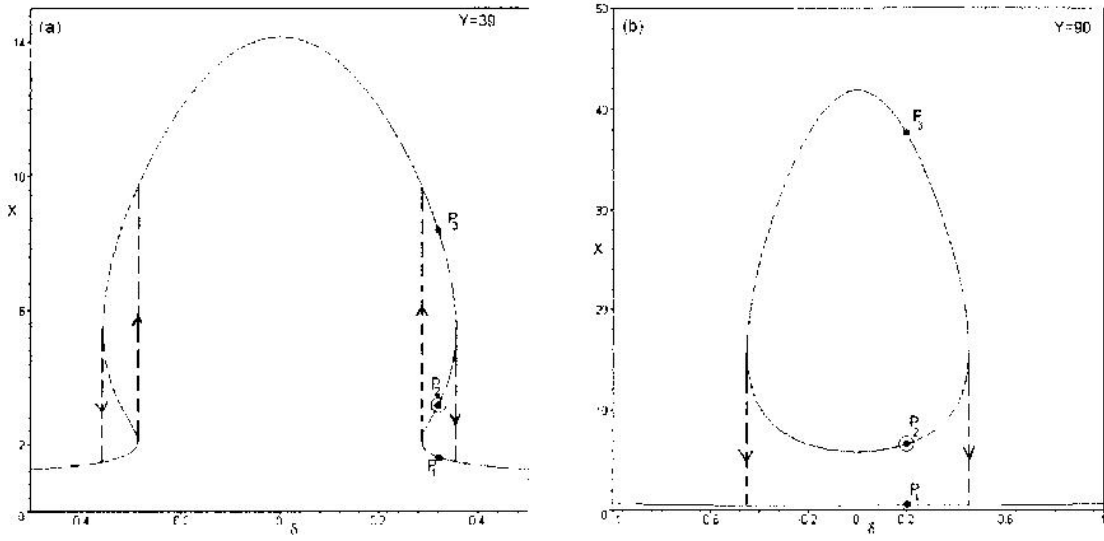
- [6] P. Galatola, L. A. Lugiato, M. G. Porro and P. Tombesi *Opt. Commun.* **81** (1991) 175.
- [7] S. S. Hassan, H. A. Batarfi, R. Saunders and R. K. Bullough, *Eur. Phys. J. D* **8** (2000) 403.
- [8] M. Benassi, F. Casagrande and W. Lange, *Quantum and Semiclass. Opt.* **9** (1997) 879.
- [9] S. S. Hassan and Y. A. Sharaby, *J. Opt. B: Quantum Semiclass. Opt.* **7** (2005) S 682.
- [10] M. F. Ali, S. S. Hassan and S. M. Maize, *J. Opt. B: Quantum and Semiclass. Opt.* **4** (2002) 388.



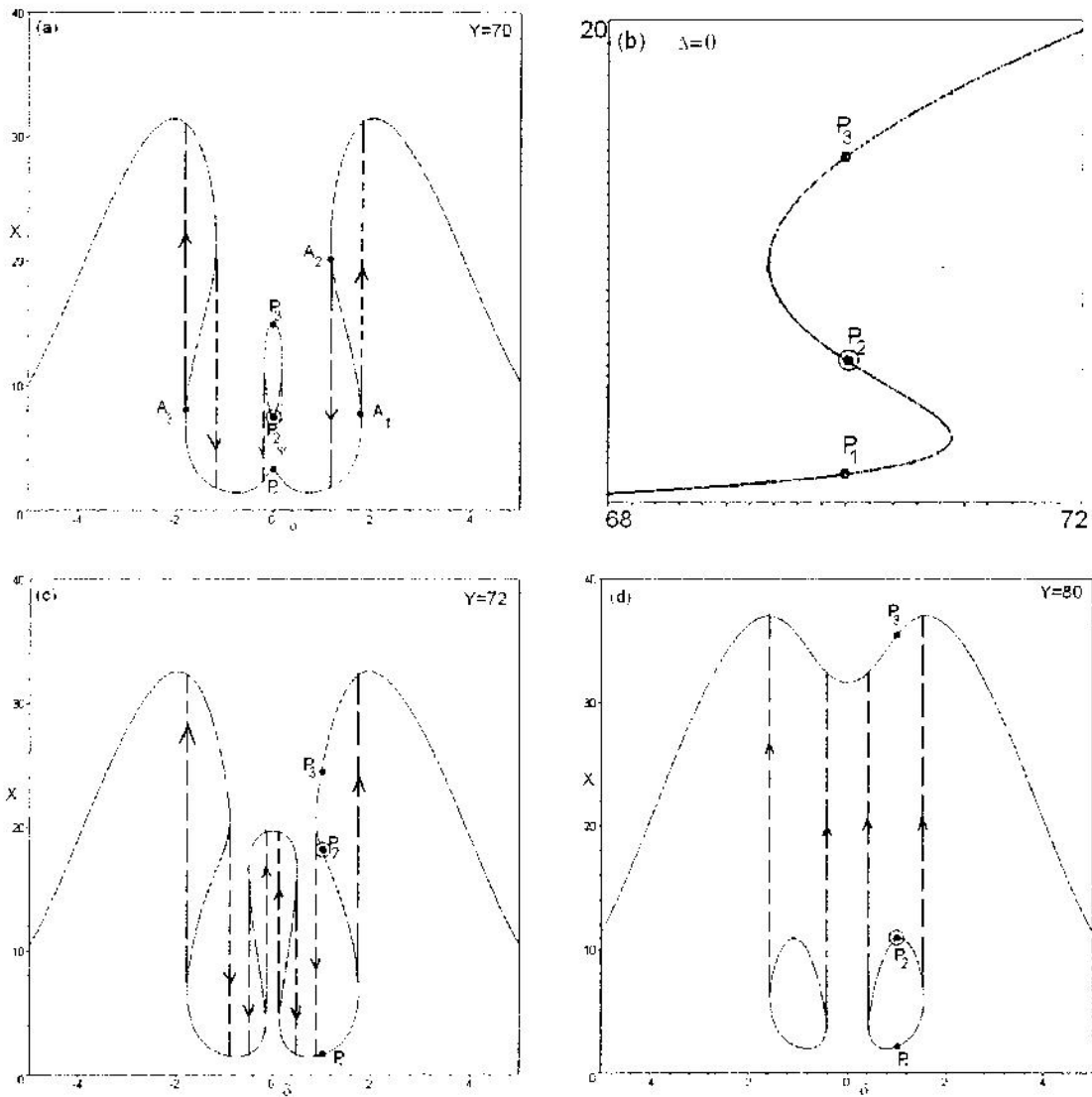
Figure(1): For $\theta = \delta$ and $C=5$, (a)the three dimensional $(\delta - X - Y)$ -plot, (b)the $(\delta-X)$ -contour plot at $Y=35$ and (c)the optical bistable behaviour for $\delta=0.5$.



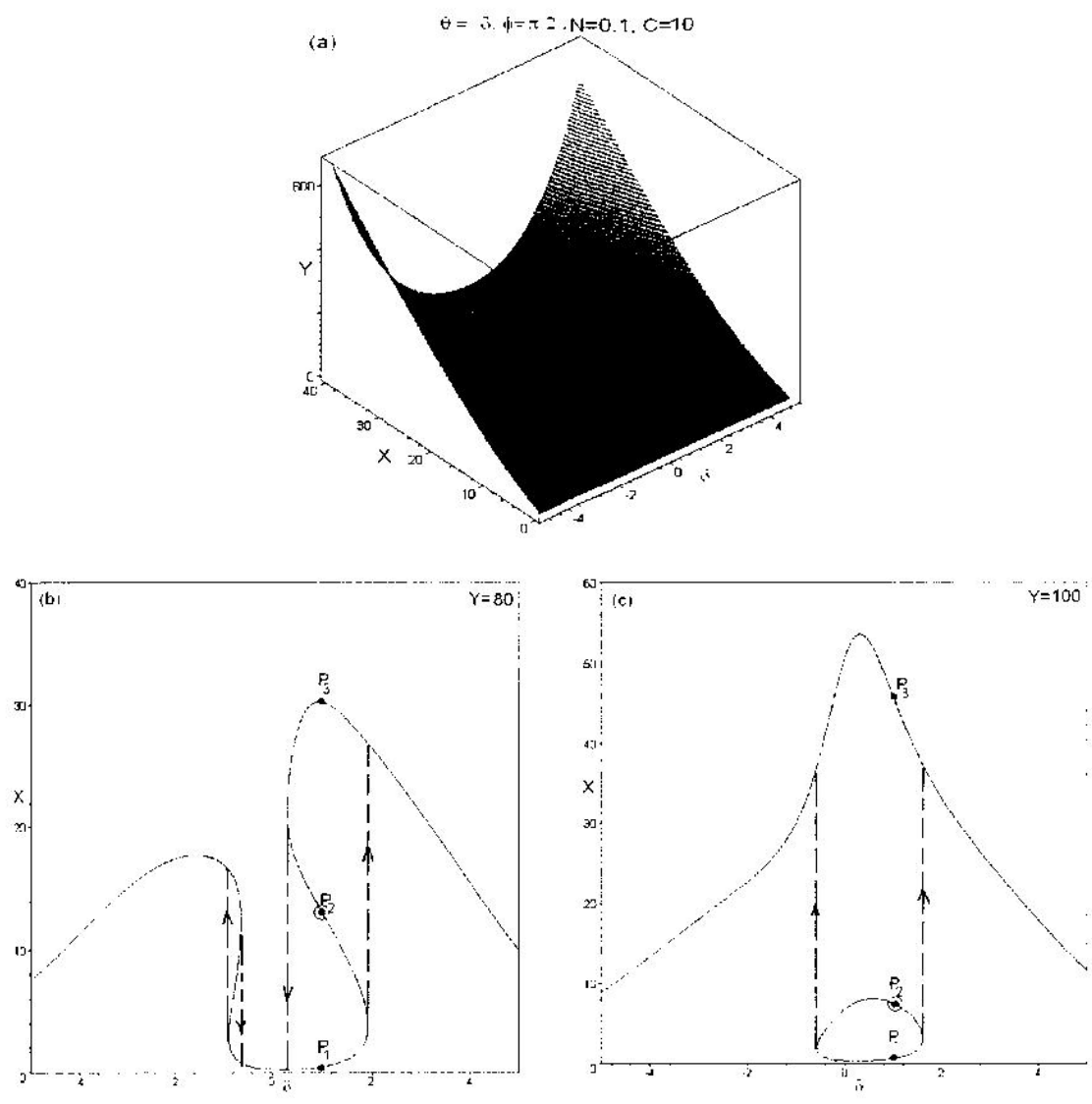
Figure(2): For $\theta = \delta$ and $C=10$, (a)the three dimensional $(\delta - X - Y)$ -plot, (b)the $(\delta-X)$ -contour plot at $Y=90$ and (c)the optical bistable behaviour for $\delta=0.5$.



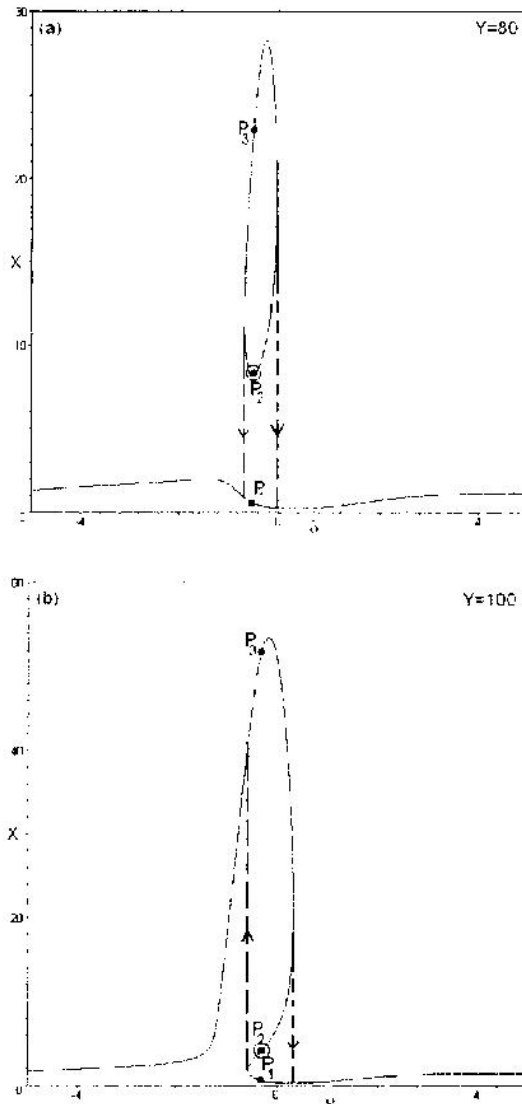
Figure(3): For $\theta = -\delta$, the (δ, X) -contour plot at (a) $C=5$, $Y=39$ and (b) $C=10$, $Y=90$.



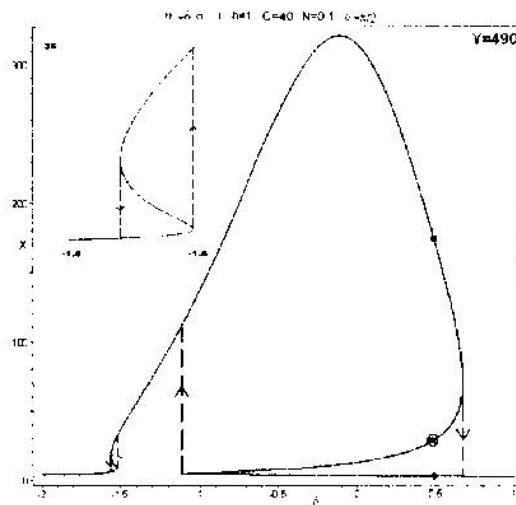
Figure(4): For $\theta = \delta$, $\phi = 0$, $N = 0.1$ and $C=10$, the $(\delta-X)$ -contour plot at (a) $Y=70$ and (b) the optical bistable behaviour for $\delta=0$, the contours at (c) $Y=72$ and (d) $Y=80$



Figure(5): For $\theta = \delta, \phi = \pi/2, N = 0.1$ and $C=10$, (a)the three dimensional $(\delta - X - Y)$ -plot, the $(\delta-X)$ -contour plot at (b) $Y=80$, (c) $Y=100$



Figure(6): For $\theta = -\delta$, $\phi = \pi/2$, $N = 0.1$ and $C=10$,
the $(\delta-X)$ -contour plot at (a) $Y=80$ and (b) $Y=100$



Figure(7): A contour at $Y=490$, $\sigma^l = 1$, $N = 0.1$, $C = 40$, $\theta = -\delta$, $\phi = \frac{\pi}{2}$
 (inset zooming view for $-1.6 \leq \delta \leq -1.5$).